

# Retention Characteristics of Five-Layered Aurivillius Films With Large Polarization

Dongpo Song,\* Jie Yang, Yuxing Wang, Liangyu Chen, Yanqiu Chu, Jie Yang, and Xuebin Zhu

The value of  $2P_r$  (twice the polarization at zero electric field) in the five-layered Aurivillius film  $\text{Bi}_6\text{Fe}_2\text{Ti}_3\text{O}_{18}$  is greater than  $50 \mu\text{C cm}^{-2}$ , which is almost an order of magnitude higher than that of the bulk ( $4 \mu\text{C cm}^{-2}$ ). Moreover, the well-defined hysteresis loop of this film can persist at the measurement frequency of 100 kHz, indicating the ultra-fast switching speed of such a domain. The frequency dependence of the coercive field obeys a power-law form,  $E_c(f) = sf^{d/\alpha}$ , indicating that its domain switching kinetics are influenced by the motion of the domain wall. The polarization of the  $\text{Bi}_6\text{Fe}_2\text{Ti}_3\text{O}_{18}$  thin film remains essentially constant at a waiting time of up to  $2 \times 10^4$  s, and is independent of the applied electric field. The switchable polarization loss is 32% after  $9 \times 10^{10}$  read/write switching cycles at a frequency of 1 MHz. This change in the switchable polarization is discussed in terms of the aggregation of oxygen vacancies in the film.

Aurivillius compounds, with the general formula  $(\text{Bi}_2\text{O}_2)^{2+}(\text{A}_{n-1}\text{B}_n\text{O}_{3n+1})^{2-}$  (where A = Na, K, Ca, Sr, Ba, Pb, Bi, etc., and B = Ti, Fe, etc.), have a naturally-layered crystal structure consisting of perovskite-like  $(\text{A}_{n-1}\text{B}_n\text{O}_{3n+1})^{2-}$  layers interleaved between fluorite-like  $(\text{Bi}_2\text{O}_2)^{2+}$  layers, where  $n$  refers to the number of perovskite-like layers.<sup>[1]</sup> The origin of ferroelectricity in the Aurivillius compounds is suggested to be due to a combination of octahedral rotations and polar distortions.<sup>[2]</sup> Owing to their fatigue-free behavior, good retention characteristics, and low leakage currents,  $\text{SrBi}_2\text{Ta}_2\text{O}_9$ -base ( $n=2$ ) Aurivillius compounds have been commercialized in ferroelectric random access memory (FeRAM) applications.<sup>[3]</sup> However, the use of  $\text{Bi}_4\text{Ti}_3\text{O}_{12}$  ( $n=3$ ) ferroelectrics has revealed a serious fatigue problem. Extensive, in-depth research on this topic has revealed that the substitution of Bi with rare-earth ions can resolve the aforementioned problem.<sup>[4]</sup> Recently, much attention has been paid to Aurivillius ferroelectrics with a high  $n$  ( $n \geq 4$ ) due to their potential for applications in room temperature

multiferroics. These ferroelectrics not only exhibit spontaneous polarization but also show magnetic ordering.<sup>[5]</sup> The coexistence of ferromagnetism and ferroelectricity has been observed in doped and un-doped Aurivillius compounds with  $n \geq 4$ , at ambient temperature and pressure.<sup>[6,7]</sup> It has been proposed that the origin of this magnetism is based on the spin canting of magnetic sublattices via the Dzyaloshinskii-Moriya interaction.<sup>[8]</sup> Theoretical studies have suggested that a higher concentration of magnetic ions would be desirable achieving robust magnetic ordering above room temperature.<sup>[9]</sup> Hence, significant research has been pursued on the structural, magnetic, and multiferroic properties of the Aurivillius compounds with  $n=5$ .<sup>[10–13]</sup> However, the ferroelectric properties of such  $n=5$  Aurivillius compounds have received lesser attention as compared to the magnetic properties, the obtained ferroelectric hysteresis loop is not saturated with slanted feature. This has been an obstacle to further investigation into the fatigue and retention properties of the Aurivillius compounds with higher  $n$ , resulting in very few reports on this subject. It is known that the ferroelectric retention and fatigue properties can play a key role in determining the performance and lifetime of ferroelectric-based devices, such as FeRAM, actuators, and microwave electronic components.<sup>[14]</sup> Therefore, it is important to investigate the ferroelectric retention and fatigue properties of  $n=5$  Aurivillius compounds for their use in FeRAM and for future applications of multiferroics.

In this study, chemical solution deposition was used to obtain  $\text{Bi}_6\text{Fe}_2\text{Ti}_3\text{O}_{18}$  thin films with a well-defined ferroelectric-hysteresis loop. The ferroelectric polarization, fatigue properties, and retention characteristics of the  $\text{Bi}_6\text{Fe}_2\text{Ti}_3\text{O}_{18}$  thin films were investigated. The influence of the applied electric field on the retention properties of these thin films was also investigated. The  $2P_r$  value of the  $\text{Bi}_6\text{Fe}_2\text{Ti}_3\text{O}_{18}$  capacitor was greater than  $50 \mu\text{C cm}^{-2}$  prior to electrical breakdown, and the well-defined ferroelectric hysteresis loop persisted up to a measurement frequency of 100 kHz. Although the switchable polarization loss did occur after the read/write switching cycles, favorable retention properties were observed, as evidenced by the fact that the polarization remained constant up to a waiting time of  $2 \times 10^4$  s and was independent of the applied electric field. The results are encouraging for the use of high  $n$ -layer structured Aurivillius films in FeRAM applications, and can serve as a

Dr. D. Song, Dr. L. Chen, Dr. Y. Chu  
Department of Physics, Jiangsu University of Science and Technology,  
Zhenjiang 212003, P.R. China  
E-mail: dpsong@just.edu.cn

Dr. J. Yang, Prof. Y. Wang  
School of materials science and engineering, Jiangsu University of  
Science and Technology, Zhenjiang 212003, P.R. China

Prof. J. Yang, Prof. X. Zhu  
Institute of Solid State Physics, Chinese Academy of Sciences, Hefei  
230031, P.R. China

DOI: 10.1002/pssr.201700278

valuable reference for further studies on room-temperature Aurivillius single-phase multiferroics.

**Crystallography and Microstructure:** The room temperature X-ray diffraction (XRD) pattern of the BFTO thin film, plotted with the intensity in a logarithmic scale, emphasizes weak peaks, as shown in **Figure 1**. This indicates that the samples are of a single phase with no detectable secondary phases. The pattern could be indexed to an orthorhombic lattice with the space group  $B2cb$ , which was well consistent with the five-layer Aurivillius structure reported in previous studies.<sup>[8]</sup> The XRD pattern showed a random orientation with a strong intensity of the (11 11) reflection, indicating the polycrystalline nature of the obtained film. This is similar to previous reports on BFTO by Bai et al., where a (111)-orientation was demonstrated, but different from the lower- $n$  Aurivillius compounds with the (001) preferred orientation. The XRD results showed that the lattice constant,  $c$ , of the BFTO thin films, is close to 49.38 Å. The in-plane lattice constants of the derived film were  $a = 5.47$  Å and  $b = 5.45$  Å, as calculated from the XRD measurements.

**Figure 2** shows the results of high-resolution transmission electron microscopy (HRTEM) measurements, which were carried out to visualize the microscopic layered structure of BFTO and to further check the crystal structure of the derived thin films. **Figure 2(a)** clearly shows a stacked structure, with five perovskite-like layers sandwiched between two fluorite-like  $(\text{Bi}_2\text{O}_2)^{2+}$  layers. This could also be confirmed by the SAED pattern shown in **Figure 2(c)**, and was analogous to the results from other studies on Aurivillius compounds.<sup>[5]</sup> The HRTEM results showed that the lattice constant,  $c$ , of the BFTO thin film is 49.67 Å, which is close to the 49.38 Å obtained from XRD results. The in-plane lattice structure of the derived film, as shown in **Figure 2(b)**, and the corresponding cubic-like SAED pattern, as shown in **Figure 2(d)**, suggested that the in-plane lattice constants are 5.51 and 5.48 Å. These values were slightly larger than those calculated from XRD measurements. To illustrate the differences between a layered structure and an in-plane image, a structural view of the orthorhombic unit cell for Aurivillius compounds with  $n = 5$  is also shown in **Figure 2**. The results of the XRD, HRTEM, and SAED analyses suggest that

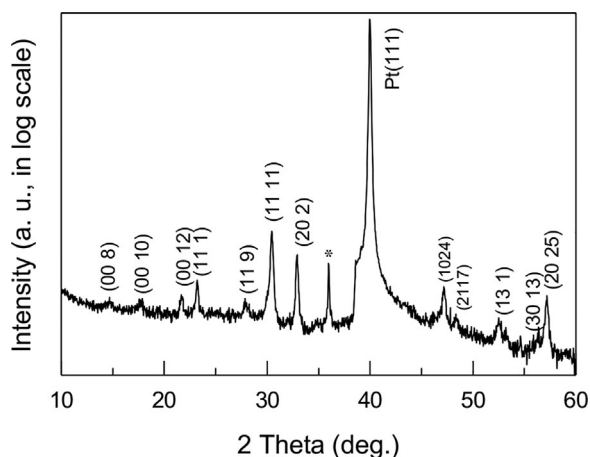


**Figure 1.** The room temperature XRD pattern of  $\text{Bi}_6\text{Fe}_2\text{Ti}_3\text{O}_{18}$  thin film. The asterisks represent the diffraction peaks from the substrates.

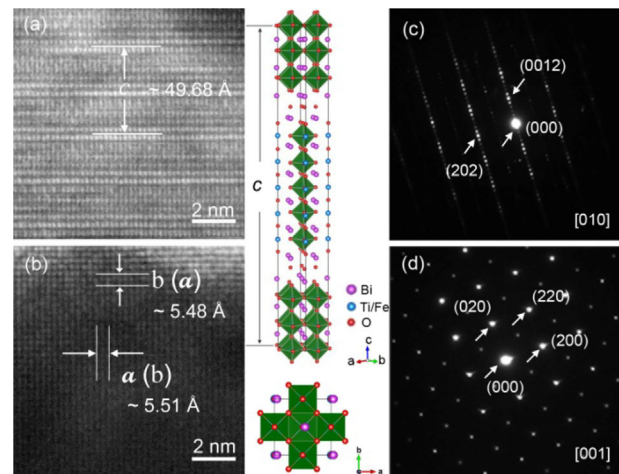


**Figure 2.** Out-of-plane (a) and in-plane (b) HRTEM microstructural analysis images of the  $\text{Bi}_6\text{Fe}_2\text{Ti}_3\text{O}_{18}$  thin film. The right side of the figure shows the corresponding SAED patterns of the (c) out-of-plane and (d) in-plane photo, respectively. The middle of the figure gives both the out-of-plane (top) and in-plane (bottom) crystal structure schematic of  $n = 5$  Aurivillius phase with an orthorhombic unit cell for clear contrast. Superlattice reflections and HRTEM measurements confirm the five perovskite-like Aurivillius phase structure.

the BFTO thin films prepared by the CSD method belong to the family of  $n = 5$  Aurivillius compounds.

**Ferroelectric Polarization Properties:** **Figure 3(a)** shows the results of polarization–electric field ( $P$ – $E$ ) measurements performed on the thin films at different applied electric fields at 5 kHz, in order to determine their polarization response. It can be seen that the BFTO thin film exhibits a well-defined ferroelectric hysteresis loop at the maximum applied electric field of  $800 \text{ kV cm}^{-1}$ , and that the  $2P_r$  ( $P_r$  is defined as the polarization at zero electric field) value can be as high as

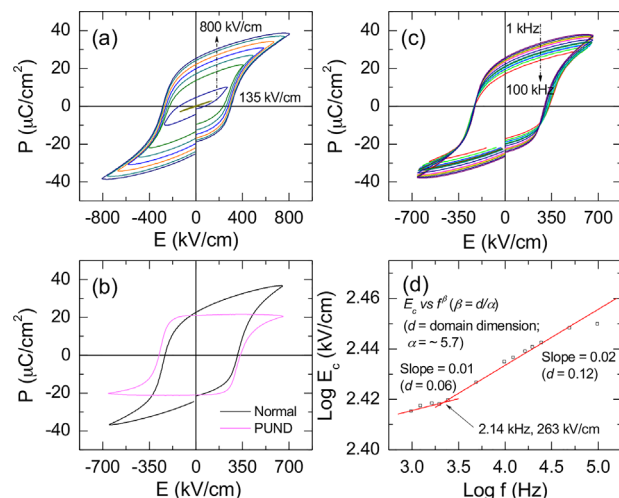


**Figure 3.** Ferroelectric polarization–electric field ( $P$ – $E$ ) hysteresis loops of  $\text{Bi}_6\text{Fe}_2\text{Ti}_3\text{O}_{18}$  thin film at room temperature measured (a) in different applied electric field at 5 kHz and (c) at different applied frequency in field of  $666 \text{ kV cm}^{-1}$ . (b)  $P$ – $E$  loops based on the normal  $P$ – $E$  measurement and the double-wave PUND method. (d) Plots of  $E_c$  versus  $f$  in the logarithmic scale. The solid lines denote the fitting results.

$50 \mu\text{C cm}^{-2}$ , which is almost an order of magnitude higher than that of the bulk ( $\approx 4 \mu\text{C cm}^{-2}$ ).<sup>[17]</sup> This value is significantly larger than the  $2P_r$  value of La-, V-, and Co-doped  $\text{Bi}_6\text{Fe}_2\text{Ti}_3\text{O}_{18}$  thin films, and is comparable to that of rare-earth-substituted  $\text{Bi}_4\text{Ti}_3\text{O}_{12}$  thin films, which have been widely studied as candidates for lead-free ferroelectrics and components of nonvolatile FeRAM.<sup>[18–20]</sup> Considering that large, anisotropic, spontaneous polarization exists in the Aurivillius compounds, the enhanced ferroelectric properties of the thin films described in this manuscript could be attributed to their predominant (111) orientation and dense morphology. It should be noted that a well-defined  $P$ - $E$  hysteresis loop can be obtained when these films are subjected to an applied electric field beyond  $400 \text{ kV cm}^{-1}$ , as shown in Figure 3(a). Further, no remnant polarization or high-leaky characteristics were observed for the BFTO thin films at  $400 \text{ kV cm}^{-1}$  in previous studies.<sup>[7,18]</sup> Given the strict definition of ferroelectricity, the contribution of the leakage current on the remnant polarization,  $2P_r$ , of the as-deposited BFTO thin film was investigated using the so-called double-wave positive-up-negative-down (PUND) pulsed polarization measurements.<sup>[21]</sup> The  $2P_r$  values obtained from the PUND measurements and the conventional  $P$ - $E$  measurements discussed above were found to be comparable. For example, the PUND  $P$ - $E$  loop in an applied field of  $666 \text{ kV cm}^{-1}$  at  $5 \text{ kHz}$  is shown in Figure 3(b). The conventional  $P$ - $E$  loop, with same applied electric field and frequency, is also shown for comparison. The difference between the  $2P_r$  (from conventional  $P$ - $E$ ) and  $2P_r$  (from PUND  $P$ - $E$ ) values is only 8%, implying that the contribution of the leakage current to the remnant polarization is insignificant.

Figure 3(c) shows  $P$ - $E$  loops at the same applied field but at different frequencies. The remnant polarization,  $2P_r$ , of the thin film decreased from  $51.2$  to  $35.2 \mu\text{C cm}^{-2}$  when the frequency was increased from  $1$  to  $100 \text{ kHz}$ . Although the remnant polarization showed a sustained downward trend, the rectangular nature of the ferroelectric loop was retained. This frequency-dependent behavior is also observed in other ferroelectrics prepared by the CSD method and is caused by the variation in the coercive fields as a function of the frequency.<sup>[13,22]</sup> Because of the slight offsets in the measured  $P$ - $E$  hysteresis loops, the experimental  $E_c$  values were determined using  $E_c = (E_c^+ - E_c^-)/2$ , where  $E_c^+$  and  $E_c^-$  are the magnitudes of the positive and negative electric fields, respectively, at zero polarization. The small offsets in the applied-field were, potentially, either due to the built-in electric fields in the ferroelectric films or the difference in electrode workfunctions.<sup>[23]</sup> Figure 3(d) shows the  $E_c$  versus  $f$  plot for the thin films, in the logarithmic scale. It can be seen that  $E_c$  increases with an increase in  $f$ , leading to lower polarization at a constant applied field. The linear fit of the  $\log(E_c)$  versus  $\log(f)$  plot in Figure 3(d) obeys the relationship  $V_c \propto f^\beta$ . This follows the domain switching model proposed by Scott, whereby the switching kinetics are influenced by the domain wall motion.<sup>[24]</sup> The value of  $\beta$  near  $2 \text{ kHz}$  changes from  $0.01$  to  $0.02$ , indicating a change in the dimensionality of the domain,  $d$ . Meanwhile, a small  $d$  value, as shown in the Figure 2(d), indicates that the energy loss caused by the hysteresis of the ferroelectrics, is low.<sup>[25]</sup>

**Fatigue and Retention Properties:** Ferroelectric fatigue and retention properties play a key role in determining the performance and lifetime of ferroelectric-based devices. The

fatigue and retention properties of the BFTO films can be studied using the saturated hysteresis loop. Ferroelectric fatigue is the primary damage mechanism by which a ferroelectric sample, undergoing repeated switching, tends to lose available remnant polarization as switching proceeds. Figure 4 shows the fatigue-endurance and charge-retention characteristics of the BFTO thin films. The symbols  $\pm P_{sw}$  and  $\pm P_{ns}$  represent the switched polarization between two opposite polarity pulses and the non-switched polarization between two similar polarity pulses, respectively. Therefore,  $\Delta P = P_{sw} - P_{ns}$  (or  $-P_{sw} - P_{ns}$ ), denotes the switchable polarization, which is an important parameter for nonvolatile memory applications. The hysteresis loops in Figure 4(a) are acquired before and after  $9 \times 10^{10}$  read/write switching cycles. Figure 4(b) shows the electrical fatigue, determined using bipolar pulses of  $8 \text{ V}$  and a test voltage of  $12 \text{ V}$  at  $1 \text{ MHz}$ . The values of  $2P_r$  and  $E_c$ , before the fatigue test, are  $\approx 37 \mu\text{C cm}^{-2}$  and  $\approx 254 \text{ kV cm}^{-1}$ , respectively. After the sample is subjected to  $9 \times 10^{10}$  cycles, the  $2P_r$  and  $E_c$  values remain relatively larger, at  $\approx 25.4 \mu\text{C cm}^{-2}$  and  $\approx 224 \text{ kV cm}^{-1}$ , respectively. Several ferroelectric fatigue mechanisms have been proposed, including charge injection,<sup>[26]</sup> defect redistribution,<sup>[27]</sup> and local phase decomposition.<sup>[14]</sup> The first two of these models are related to the variation of charged defects. XPS measurements, presented above, have demonstrated the coexistence of  $\text{Fe}^{2+}$  and  $\text{Fe}^{3+}$  in the BFTO films, indicating that the generation of charged defects, such as oxygen vacancies ( $V_O$ ), is inevitable during the annealing process.<sup>[3]</sup> In lower  $n=2$  Aurivillius ferroelectrics, such as SBT ( $\text{SrBi}_2\text{Ta}_2\text{O}_9$ ), excellent sustainability of ferroelectricity is observed, even with the presence of oxygen vacancies. This resistance to fatigue in SBT is attributed to a space charge compensation mechanism near the electrodes, by the bismuth oxide double layers. When  $n$  increases to three, for example  $\text{Bi}_4\text{Ti}_3\text{O}_{12}$ , the typical fatigue failure is observed due to the differences in the nature of the  $V_O$  defect between  $n=2$  and  $3$ . This is because the oxygen vacancies can be induced at both

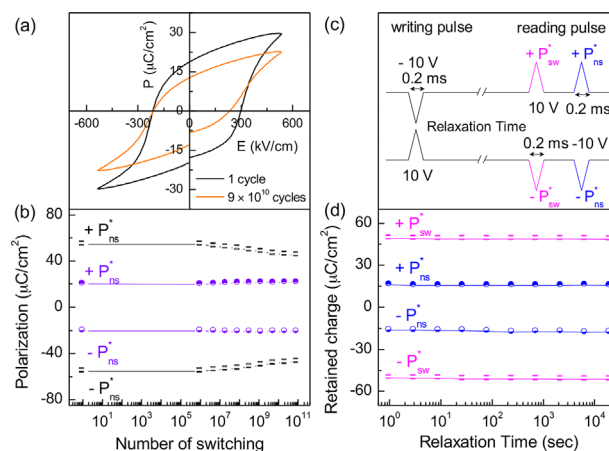


**Figure 4.** Charge-retentions and fatigue characteristics of  $\text{Bi}_6\text{Fe}_2\text{Ti}_3\text{O}_{18}$  thin film at room temperature. (a)  $P$ - $E$  hysteresis loops measured in a voltage of  $12 \text{ V}$  before and after  $9 \times 10^{10}$  read/write switching cycles. (b) Fatigue-test results determined with a switching voltage of  $8 \text{ V}$  and a measuring voltage of  $12 \text{ V}$  at a frequency of  $1 \text{ MHz}$ . Panel (c) represents two distinctive test-pulse sequences and (d) shows the retention time dependence of the retained polarization.

the titanium-oxygen octahedra and the  $(\text{Bi}_2\text{O}_2)^{2+}$  layers. In SBT, on the other hand, the oxygen ions at the perovskite-like layers are much more stable than those at the  $(\text{Bi}_2\text{O}_2)^{2+}$  layers.<sup>[28]</sup> Moreover, the fatigue-resistant behavior of SBT is more likely due to the fact that Ti and Fe are multivalent (i.e., easy to change from one oxidation state to another), while Ta is not. For the  $\text{Bi}_6\text{Fe}_2\text{Ti}_3\text{O}_{18}$  ( $n = 5$ ), the role of  $V_{\text{O}}$  may be similar to that in the  $\text{Bi}_4\text{Ti}_3\text{O}_{12}$  because more perovskite-like layers are involved and simple perovskite-typed ferroelectrics are usually less tolerant to oxygen vacancies.<sup>[29]</sup> Such differences in the nature of  $V_{\text{O}}$  may be responsible for the fatigue behavior observed in the thin films in the present study. However, the larger switchable polarization was found to be reserved up to  $9 \times 10^{10}$  cycles, suggesting that BFTO can be a potential candidate for memory applications.

Retention is defined as the ability to maintain remnant polarization, in a given polarization state, for an extended period of time. The charge-retention characteristic of the BFTO capacitor is shown in Figure 4 (right-hand side), by plotting  $\pm P_{\text{sw}}$  and  $\pm P_{\text{ns}}$  as a function of time. The test pulse sequence used for retention measurement is given in Figure 4(c) as follows:  $+P_{\text{sw}} + P_{\text{ns}} \rightarrow -P_{\text{sw}} - P_{\text{ns}}$ . First, a negative pulse of 10 V was applied to write a known logic state. Next, the logic state was sequentially read by applying two triangular pulses of +10 V (or -10 V) after a predetermined time interval. The pulse width was 0.2 ms, and the interval time was 1 s. Figure 4(d) shows the retention characteristics of the BFTO film. Both polarizations approached a near steady-state value after a retention time of  $2 \times 10^4$  s, implying that the retained switchable polarization is stable. This strongly suggests that BFTO films have large values of  $(P_{\text{sw}} - P_{\text{ns}})$  and good retention ability.

To further characterize the retention properties of the BFTO films, measurements of  $+P_{\text{sw}}$  and  $+P_{\text{ns}}$  were performed as a function of time, in different electric fields. The field-dependent retention of the BFTO thin films showed minimal change, as seen in Figure 5, suggesting that the retention properties of these films are insensitive to the applied field. The corresponding

hysteresis loops before and after the retention test were almost identical, which further confirms that there was almost no loss in the switchable polarization. Even after a retention time of  $2 \times 10^4$  s, the polarization loss was insignificant as compared to the value measured at  $t = 1$  s, under a constant electric field. Depolarization fields are usually considered to be the mechanism for the polarization decay after writing, which could be caused either by the defects and dipole charges or by the redistribution of space charges.<sup>[30]</sup> Typically, the long-term retention loss is attributed to the effects of charged defects,  $V_{\text{O}}$ . However, this effect leads only to a small decrease in the polarization of BFTO thin films, due to the compensation for these charges by the redistribution of the defects, driven by the polarization.<sup>[31]</sup> In BFTO films, the larger switched charges may help suppress the negative effects of the charged defects on the polarization loss during the retention times.

In conclusion, ferroelectric  $\text{Bi}_6\text{Fe}_2\text{Ti}_3\text{O}_{18}$  thin films were prepared on platinum-coated silicon substrates by chemical solution deposition, and their ferroelectric and retention properties were investigated in detail. The value of  $2P_r$  was measured to be greater than  $50 \mu\text{C cm}^{-2}$ , which is almost an order of magnitude higher than that of the bulk ( $4 \mu\text{C cm}^{-2}$ ). The remnant polarization was found to decrease with increasing frequency and a well-defined ferroelectric hysteresis loop persisted in the measurement frequency of 100 kHz, indicating the ultra-fast switching speed of such domains. Fatigue behavior was attributed to the appearance of oxygen vacancies, arising from the coexistence of  $\text{Fe}^{2+}$  and  $\text{Fe}^{3+}$  in the films. Favorable retention properties were observed, as evidenced by the fact that the polarization remained constant at a waiting time of up to  $2 \times 10^4$  s, and was independent of the applied electric field. The results demonstrate that the overall retention time and field-independence of polarization of BFTO thin films makes them favorable for memory applications.

## Experimental Section

Ambient atmosphere chemical solution deposition (CSD), combined with rapid annealing, was used to deposit thin films of  $\text{Bi}_6\text{Fe}_2\text{Ti}_3\text{O}_{18}$  (BFTO) on polycrystalline Pt/Ti/SiO<sub>2</sub>/Si (100) substrates. The precursor solution used for the coating was prepared by dissolving appropriate amounts of high-purity bismuth acetate, iron acetate, and tetrabutyl titanate in propanoic acid. Details of the solution preparation and coating have been reported previously.<sup>[15,16]</sup> The thin film was spin-coated at 6000 rpm for 20 s and then baked in a 400 °C preheated tube furnace for 10 min in air. The process of spin-coating and pyrolysis was repeated several times to obtain a film thickness of  $\approx 225$  nm measured by field emission scanning electron microscopy (FE-SEM). The dried amorphous film was subsequently crystallized in a tube furnace for 0.5 h at 700 °C. The as-derived film was sheeny and crack-free, and adhered well to the substrate. The crystal structure of the film was determined with a Philips X'Pert PRO X-ray diffractometer (XRD) with Cu-K $\alpha$  radiation, at room-temperature. High-resolution transmission electron microscopy (HRTEM) images and selected-area electron diffraction (SAED) patterns were obtained using a transmission electron microscope (TEM, JEM-2010, JEOL Ltd., Japan). The surface morphology and thickness of the films were examined using a field-emission scanning electron microscope (FE-SEM, Sirion 200, FEI Company, USA). The ferroelectric properties were measured using a Sawyer-Tower circuit attached to a computer-controlled standardized ferroelectric test system (Precision Premier II, Radiant Technology, USA). Top Au electrodes with a diameter of 0.2 mm were sputtered on the film to measure the electrical properties.

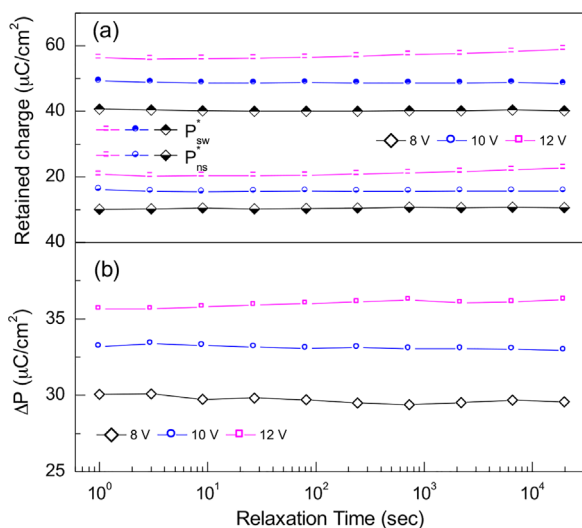


**Figure 5.** Retention time dependence of (a) the charge retentions and (b) retained switchable polarization of  $\text{Bi}_6\text{Fe}_2\text{Ti}_3\text{O}_{18}$  thin film at room temperature in various applied electric fields.

## Acknowledgements

This work was supported by the Joint Funds of the National NSFC (Grant Nos. U1432137), the Natural Science Foundation of the Higher Education Institutions of Jiangsu Province (17KJB140006), the Scientific Research Foundation of Jiangsu University of Science and Technology (Nos. 1052931611).

## Conflict of Interest

The authors declare no conflict of interest.

## Keywords

Aurivillius compounds, ferroelectrics, oxides, thin films

Received: August 17, 2017

Revised: September 10, 2017

Published online: September 22, 2017

- 
- [1] E. C. Subbarao, *J. Phys. Chem. Solids* **1962**, 23, 665.  
 [2] N. A. Benedek, *Inorg. Chem.* **2014**, 53, 3769.  
 [3] J. F. Scott, *Science* **2007**, 315, 954.  
 [4] B. H. Park, B. S. Kang, S. D. Bu, T. W. Noh, J. Lee, W. Jo, *Nature* **1999**, 401, 682.  
 [5] L. Keeney, T. Maity, M. Schmidt, A. Amann, N. Deepak, N. Petkov, S. Roy, M. E. Pemble, R. W. Whatmore, D. Johnson, *J. Am. Ceram. Soc.* **2013**, 96, 2339.  
 [6] H. Y. Zhao, H. Kimura, Z. X. Cheng, M. Osada, J. L. Wang, X. L. Wang, S. X. Dou, Y. Liu, J. D. Yu, T. Matsumoto, T. Tohei, N. Shibata, Y. Ikuhara, *Sci. Rep.* **2014**, 4, 5255.  
 [7] W. Bai, W. F. Xu, J. Wu, J. Y. Zhu, G. Chen, J. Yang, T. Lin, X. J. Meng, X. D. Tang, J. H. Chu, *Thin Solid Films* **2012**, 525, 195.  
 [8] J. Yang, W. Tong, Z. Liu, X. B. Zhu, J. M. Dai, W. H. Song, Z. R. Yang, Y. P. Sun, *Phys. Rev. B* **2012**, 86, 104410.  
 [9] A. Y. Birenbaum, C. Ederer, *Phys. Rev. B* **2014**, 90, 214109.  
 [10] E. Jartych, T. Pikula, M. Mazurek, A. Lisinska-Czekaj, D. Czekaj, K. Gaska, J. Przewoznik, C. Kapusta, Z. Surowiec, *J. Magn. Magn. Mater.* **2013**, 342, 27.  
 [11] J. Yang, L. H. Yin, Z. Liu, X. B. Zhu, W. H. Song, J. M. Dai, Z. R. Yang, Y. P. Sun, *Appl. Phys. Lett.* **2012**, 101, 012402.  
 [12] J. L. Wang, H. L. Huang, C. H. Liu, Z. P. Fu, X. F. Zhai, R. R. Peng, Y. L. Lu, *Appl. Phys. Lett.* **2015**, 106, 132903.  
 [13] H. Sun, B. W. Zou, X. R. Ni, X. Y. Mao, X. B. Chen, J. G. Zhu, *J. Mater. Sci.* **2015**, 50, 5475.  
 [14] X. J. Lou, M. Zhang, S. A. T. Redfern, J. F. Scott, *Phys. Rev. B* **2007**, 75, 224104.  
 [15] D. P. Song, X. W. Tang, B. Yuan, X. Z. Zuo, J. Yang, L. Chen, W. H. Song, X. B. Zhu, Y. P. Sun, *J. Am. Ceram. Soc.* **2014**, 97, 3857.  
 [16] D. P. Song, X. Z. Zuo, B. Yuan, X. W. Tang, W. H. Song, J. Yang, X. B. Zhu, Y. P. Sun, *CrystEngComm* **2015**, 17, 1609.  
 [17] X. Z. Zuo, J. Yang, D. P. Song, B. Yuan, X. W. Tang, K. J. Zhang, X. B. Zhu, W. H. Song, J. M. Dai, Y. P. Sun, *J. Appl. Phys.* **2014**, 116, 154102.  
 [18] C. M. Raghavan, J. W. Kim, J.-W. Kim, S. S. Kim, *Ceram. Int.* **2014**, 40, 10649.  
 [19] Z. Liu, J. Yang, X. W. Tang, L. H. Yin, X. B. Zhu, J. M. Dai, Y. P. Sun, *Appl. Phys. Lett.* **2012**, 101, 122402.  
 [20] L. L. Jiao, Z. M. Liu, G. D. Hu, S. G. Cui, Z. J. Jin, Q. Wang, W. B. Wu, C. H. Yang, *J. Am. Ceram. Soc.* **2009**, 92, 1556.  
 [21] J. G. Wu, K. Wang, *J. Am. Ceram. Soc.* **2010**, 93, 1422.  
 [22] H. Sun, X. M. Lu, T. T. Xu, J. Su, Y. M. Jin, C. C. Ju, F. Z. Huang, J. S. Zhu, *J. Appl. Phys.* **2012**, 111, 124116.  
 [23] F. Yang, F. W. Zhang, G. D. Hu, Z. H. Zong, M. H. Tang, *Appl. Phys. Lett.* **2015**, 106, 172903.  
 [24] J. F. Scott, *Integr. Ferroelectr.* **1996**, 12, 71.  
 [25] Y. Ishibashi, H. Orihara, *Integr. Ferroelectr.* **1995**, 9, 57.  
 [26] A. K. Tagantsev, I. Stolichnov, E. L. Colla, N. Setter, *J. Appl. Phys.* **2001**, 90, 1387.  
 [27] J. F. Scott, M. Dawber, *Appl. Phys. Lett.* **2000**, 76, 3801.  
 [28] B. H. Park, S. J. Hyun, S. D. Bu, T. W. Noh, J. Lee, H.-D. Kim, T. H. Kim, W. Jo, *Appl. Phys. Lett.* **1907**, 1999, 74.  
 [29] Q. Q. Ke, A. Kumar, X. J. Lou, Y. P. Feng, K. Y. Zeng, Y. Q. Cai, J. Wang, *Acta Mater.* **2015**, 82, 190.  
 [30] A. Z. Simoes, M. A. Ramirez, N. A. Perruci, C. S. Riccardi, E. Longo, J. A. Varela, *Appl. Phys. Lett.* **2005**, 86, 112909.  
 [31] B. S. Kang, J. G. Yoon, T. K. Song, S. Seo, Y. W. So, T. W. Noh, *Jpn. J. Appl. Phys.* **2002**, 41, 5281.